

## Quiet-Sun: A Comparison of MDI and SOT Fluxes

Clare E. Parnell,<sup>1</sup> Craig E. Deforest,<sup>2</sup> Hermance J. Hagenaar,<sup>3</sup> Derek A. Lamb<sup>4</sup> and Brian T. Welsch<sup>5</sup>

<sup>1</sup>*University of St Andrews, St Andrews, Scotland*

<sup>2</sup>*Southwest Research Institute, Boulder, USA*

<sup>3</sup>*Lockheed Martin Space and Astrophysics Lab., Palo Alto, USA*

<sup>4</sup>*University of Colorado, Boulder, USA*

<sup>5</sup>*Space Sciences Lab., University of California, Berkeley, USA*

**Abstract.** The SOT-NFI on *Hinode* has both higher resolution and better sensitivity than MDI on SOHO. Line-of-sight magnetograms of the quiet Sun taken simultaneously by both MDI and SOT are investigated to show how the observed flux differs between the two instruments. We find that: (i) the total unsigned flux observed by SOT is approximately 50% greater than that observed by MDI and (ii) the total signed flux remains approximately constant. Thus, the extra flux observed by SOT is made up of equal amounts of positive and negative flux. By comparing the observed flux distributions from MDI and SOT we find that the extra flux is contained in features with fluxes less than the smallest observed by MDI. Indeed, the smallest features in SOT have just  $\geq 10^{16}$  Mx, a factor of thirty less than the smallest observed by MDI.

The distributions of feature fluxes observed by the two instruments are also compared. We find that by using a ‘clumping’ algorithm, which counts a single ‘flux massif’ as one feature, the fluxes in MDI and SOT follow the same distribution - a power-law - between  $2 \times 10^{17}$  and  $10^{20}$  Mx. Thus, the mechanism producing network and intranetwork features appears to be the same. Furthermore, the power-law index of this distribution is found to be  $-1.85$ . This value is neither the Kolomogrov  $-5/3$  slope of hydrodynamic turbulence nor the Krichenen  $-2$  slope of magneto-hydrodynamic turbulence, although both of these numbers may be within the error bars of our analysis.

## 1. Introduction

In order to understand the behaviour and origins of quiet-Sun small-scale magnetic features it is useful to identify and track flux features. However, the identification of a ‘feature’, its flux, area and position, strongly depend on the algorithm applied (DeForest et al. 2007). For example, Parnell (2002) used a clumping algorithm to identify features in MDI high-resolution data and found that the resulting distribution was best described by a Weibull. However, Hagenaar et al. (2003), used a curvature-based algorithm on similar MDI data and found a flux distribution which resembled a double exponential, suggesting that different mechanisms generate features of different scales.

The *clump* feature identification method clusters together all connected like-polarity pixels with values above a lower cutoff to form a feature, i.e., it counts ‘flux massifs’. Downhill or curvature feature identification methods identify ‘peaks’ and so find several features for each flux massif. Clearly, using data with

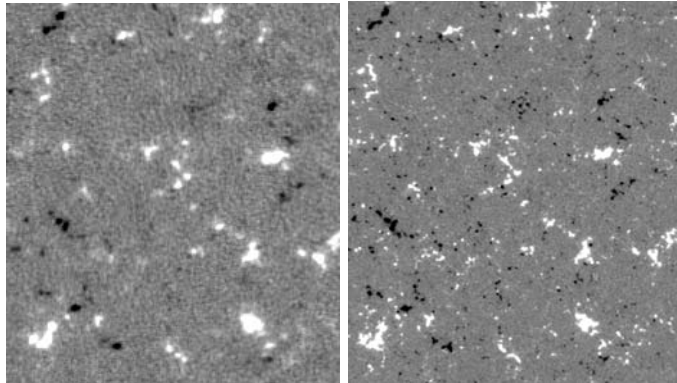


Figure 1. Sample MDI (*left*) and SOT (*right*) images showing the line-of-sight magnetic field component of the same area of quiet-Sun taken on June 24th 2007. Each image has an area of  $141 \times 161$  arcsec<sup>2</sup>.

greater resolution and sensitivity, the peak identification methods can break up flux-massifs even more. Thus, we find that the best method for comparing the distributions of fluxes from MDI and SOT-NFI is the clumping approach.

In the following, we compare the distribution of MDI and SOT fluxes to determine if either of the previous flux distribution results hold for quiet-Sun fluxes observed by SOT. We also consider how much more flux can be seen with the improved resolution and sensitivity of SOT than with MDI.

## 2. MDI and SOT data sets

MDI high resolution and SOT data sets taken simultaneously on 24th June 2007 between 22:09 and 23:08 UT were analyzed (Fig 1). Both data sets have a 1 minute cadence. The quiet-Sun area observed is near disk centre. The MDI data have pixel areas of  $0.370$  arcsec<sup>2</sup>, whilst the SOT pixel areas are about a factor 16 smaller at just  $0.026$  arcsec<sup>2</sup>. The MDI magnetograms use the Ni I  $6768\text{\AA}$  line whilst the SOT magnetograms use the Na D  $5896\text{\AA}$  line. Both data sets only include line-of-sight components of the magnetic field. At the time of analysis of the data (July/August 2007) there was no magnetic calibration available for the SOT data. To ‘calibrate’ the data we cross-correlated a five-minute-averaged blurred SOT image with the simultaneous five-minute-averaged MDI image. It was found that the 6555 SOT V/I was equal to 1 MDI Mx cm<sup>-2</sup>. For full details on the preparation and calibration of the data see Parnell et al. (2008).

## 3. Flux Distributions

As previously discussed, the clumping algorithm was used to identify features in individual frames using a lower cutoff. For the MDI and SOT data lower cutoffs of  $28\text{ Mx cm}^{-2}$  and  $18\text{ Mx cm}^{-2}$  and upper cutoffs of  $38\text{ Mx cm}^{-2}$  and  $24\text{ Mx cm}^{-2}$ , were used respectively. After identification the features were associated between frames. All features with areas less than 4 pixels were removed, as were

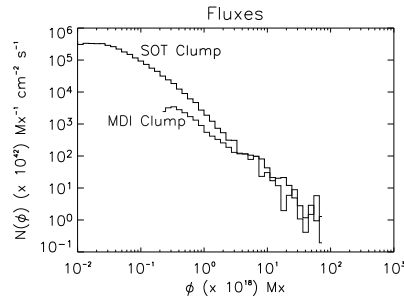


Figure 2. Log-log plot of histograms of all the MDI and SOT feature fluxes observed over our one hour of data.

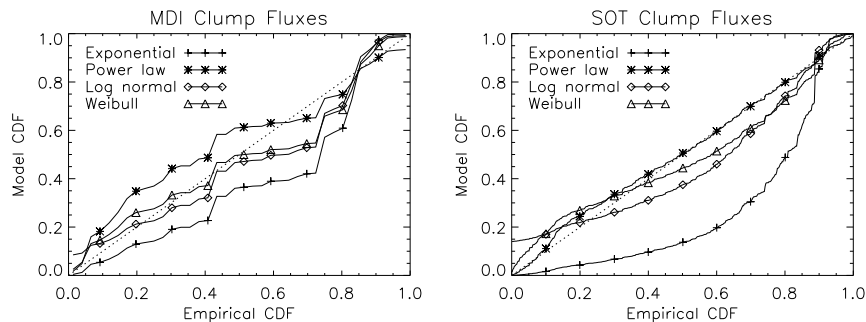


Figure 3. Sample PP plots for flux distributions in a single frame with the model cumulative distribution function (CDF) plotted against the empirical CDF. Four models are considered: exponential (+), power-law (\*), log-normal ( $\diamond$ ) and Weibull ( $\triangle$ ) with the best parameters for each model found using maximum likelihood. The line corresponding to the model that best fits the observed distribution should lie along  $x = y$  (dashed).

those that did not at sometime during their lives reach a peak greater than the upper cutoff. Features with lifetimes less than 4 minutes were removed.

Figure 2 shows histograms of the MDI and SOT fluxes for all the observed features. Clearly, the tails of the distributions appear to follow a power-law. A key question is: are the MDI and SOT distributions the same?

Due to our algorithm, features with peaks just above the lower cutoff have their fluxes underestimated (Parnell 2002) and thus the turnovers at the lower ends of the distributions may not be real. To determine the real quiet-Sun flux distribution we ignore these lower portions. Lower thresholds for the fluxes were found to be  $3.4 \times 10^{18} \text{ Mx cm}^{-2}$  and  $1.8 \times 10^{17} \text{ Mx cm}^{-2}$  for MDI and SOT, respectively. Furthermore, the flux distribution for each frame must be considered separately otherwise our results may be skewed if, for example, one strong feature has an excessively long lifetime. This leaves us with an average of just 100 or 1200 fluxes per frame for MDI and SOT. Histograms are therefore inappropriate, instead rigorous statistical methods are applied.

We test the hypothesis that our observed flux distributions follow one of four possible model distributions. PP plots compare all four models in one particular frame (e.g., Figure 3). Clearly, neither the MDI nor SOT fluxes are distributed

exponentially. From the MDI data it is hard to distinguish between any of the other three models. On the other hand it is clear from the SOT data that the power-law is the best fitting model. This result holds true for all frames. The Kolomogorov-Smirnov (KS) statistic, a one number summary of the PP plot, is used to quantify the goodness of fit of the model distributions in each frame. We find that for the MDI data, three of the model distributions are regularly classed as statistically good fits. However, the Weibull appears to be the most likely distribution since it is a statistically good fit 65% of the time and is found to be the best fitting model in 73% of the frames. This agrees with the result found in Parnell (2002). For the SOT data, only the power law is ever classed as a statistically good fit and this occurs 27% of the time. Furthermore, the power-law is found to be the best fitting model in every frame.

Comparing the indices for the best fitting MDI and SOT power-law distributions we find that both give a typical value of about  $-1.85$ . Hence, it is not unreasonable to think that the MDI and SOT distributions of feature fluxes identified using a clumping method are in fact the same - a simple power law. A power-law distribution of feature fluxes suggests that the mechanism generating flux massifs is the same on both the supergranular and granular scales.

#### 4. New Flux

We now compare the average flux per frame observed by MDI and SOT. The total absolute flux observed by MDI is  $520 \times 10^{18}$  Mx, whilst SOT observed about 50% more flux to give a total of  $774 \times 10^{18}$  Mx. The total net flux observed by MDI and SOT is approximately the same at  $356 \times 10^{18}$  Mx and  $358 \times 10^{18}$  Mx, respectively. So the extra flux consists of equal amounts of positive and negative flux, which, from the distributions, appears as many tiny features.

A recent paper by Lamb et al. (2008) shows that 90% of the new flux observed in MDI magnetograms seems to appear as ‘unipolar appearances’, suggesting that there are significant amounts of flux at the sub-MDI-resolution. This has been confirmed by this work. Moreover, preliminary results suggest that there may also be sub-SOT-resolution flux, though this needs to be confirmed.

*For a more complete discussion of all these results see Parnell et al. (2008).*

**Acknowledgments.** We thank the *Hinode*/SOT and SOHO/MDI teams for the excellent data that permitted this study and SWRI, Boulder, for hosting the 3rd Magnetic tracking workshop where this project was initiated.

#### References

- DeForest C. E., Hagenaar H. J., Lamb D. A., Parnell C. E., Welsch B. T. 2007, ApJ, 666, 576
- Hagenaar H. J., Schrijver C. J., Title A. M. 2003, ApJ, 584, 1107
- Lamb D. A., DeForest C. E., Hagenaar H. J., Parnell C. E., Welsch B. T. 2008, ApJ, 674, 520
- Parnell C. E. 2002, MNRAS, 335, 389
- Parnell C. E., DeForest C. E., Hagenaar H. J., Lamb D. A., Welsch B. T. 2008, ApJ, in preparation